2021

Compressor Performance Comparison of R454A and R454C for Refrigeration

Lars Sjoholm
Trane Technologies, Thermo King, Compressor Engineering, USA

YoungChan Ma
Trane Technologies, Thermo King, Compressor Engineering, USA,
youngchan_ma@tranetechnologies.com

Gurudath Nayak
Trane Technologies, Modeling and Simulation, India

Matt Stinson
Trane Technologies, Modeling and Simulation, USA

Compressor Performance Comparison of R454A and R454C for Refrigeration

Lars SJOHOLM[1], Young Chan MA[2*], Gurudath NAYAK[3], Matt STINSON[4]

[1] Trane Technologies — Thermo King,
Minneapolis, Minnesota, USA
Lars_Sjoholm@tranetechnologies.com

[2*] Trane Technologies — Thermo King,
Minneapolis, Minnesota, USA
Youngchan_Ma@tranetechnologies.com

[3] Trane Technologies, Modeling and Simulation,
Bengaluru, India
Gurudath.Nayak@tranetechnologies.com

[4] Trane Technologies, Modeling and Simulation,
Minneapolis, Minnesota, USA
Matthew.Stinson@tranetechnologies.com

* Corresponding Author

ABSTRACT

The intent of this paper is to compare compressor performance of two low GWP refrigerants that are mildly flammable. Since there are limited test capabilities for compressors with flammable refrigerants, the compressor tests in this paper are based on a non-flammable refrigerant, in this case R513A. The tested compressor is an open type screw compressor that is driven by an external motor and is vapor injected. A physical compressor model is created from test data. This compressor model is not based on maps for efficiencies, capacity, or power consumption, but rather a basis of physical bulk elements, such as pressure drop from orifices (at suction, discharge and vapor injection), leakage orifices, volume ratio between the suction port and the vapor injection port as well as volume ratio between the suction port and the discharge port. The compressor displacement and speeds are the most fundamental inputs for both the model and the tests. For mechanical losses a friction coefficient and friction exponent, relative to the speed, are obtained from the developed compressor model. This model can predict the actual compressor operation with different refrigerants. This compressor model developed based on R513A testing is applied to predict the performance of R454A and R454C refrigerants that are potential candidates for low GWP transport refrigeration. R454A always gives higher capacity than R454C. For COP, R454A outperforms R454C in some conditions while R454C outperforms R454A in others.

1. INTRODUCTION

When looking at many different refrigerants, especially A2L or mildly flammable, the use of compressor modelling and simulations becomes very important in early development because there are limited testing capability available for flammable refrigerants. Standard compressor rating models (AHRI, 2020), where refrigeration capacity and power consumption are curve fitted, would not work. The traditional approach would be to use some kind of compressor efficiency model (Cambio, 2016; Erickson, 1998; Sjoholm & Ma, 2018). Furthermore, the isentropic efficiency is hard to define for a vapor injected compressor due to the assumed mixing behavior between the main suction flow and the vapor injection flow. Another approach would be to use a one dimensional physical model, where the model is driven by the geometry of the compressor. The problem with such a model is that it still needs some correlation between simulation and test. The model used in this paper, is a physical model based on bulk elements that is test data driven directly. This way no special correlation procedure is needed. To use this physical model, at least in theory, it should be very good for different refrigerants assuming that the model is a good representation of the compressor. CFD models are not efficient because of very different grid representation in flow zones and tight clearance zones. Besides this, the compressor model has to handle economizer flow or vapor injection. To model this with good results

is challenging because the vapor injection port is open to a relative large part of the volume curve. This makes it hard to define the vapor injection port as a positive displacement port. The larger the operating range is, regarding pressures, temperatures, and speed, the harder it is to predict this flow.

The objective of this paper is not to show what refrigerant is better between R454A and R454C. Rather, it is to show some thermodynamic behavior differences. To figure out what refrigerant best suits a certain application, the whole refrigeration system and the user profiles have to be taken into account.

2. LOW GWP REFRIGERANTS

The target refrigerants for this study are R454A and R454C. The other refrigerants R32, R452B, R454B and R466A are excluded due to too high discharge temperature. R1234yf, R1234ze, R513A, and other R134a like refrigerants are excluded due to too low suction pressure. Any refrigerant blends with R1234ze, R13I1 and R744 as components are not considered due to their different or unknown behaviors. No components based on A2 or A3 were considered. The desired GWP should be below 700 or 150. Some basic data for R454A and R454C are shown on Table 1.

Table 1: The Basic Data for R454A and R454C

ASHRAE Designation	ASHRAE Class	GWP (AR4)	R32	R1234yf	Molecular Weight	Normal Bubble Point	Normal Dew Point	Critical Temperature	Critical Pressure
			Mass Fraction		g/mol	°C	°C	°C	kPa
R454A	A2L	239	0.350	0.650	80.468	−48.33	−41.61	85.72	4900.8
R454C	A2L	148	0.215	0.785	90.776	−45.89	−37.72	88.50	4474.0

Two temperature reference points are selected for this study. For low temperature refrigeration, −35/40 °C (suction dew temperature/discharge dew temperature) is chosen and medium temperature refrigeration −10/45 °C is chosen (AHRI, 2020). Table 2 shows the temperature glide at the selected temperatures and the two refrigerants. Hundy & Vittal (2000) discusses handling the glide effects on compressor performance definitions.

Table 2: The Temperature Glide Comparison of R454A and R454C

Dew Temperature	R454A		R454C	
	Pressure	Temperature Glide	Pressure	Temperature Glide
°C	kPa	K	kPa	K
−35	141.53	5.71	115.11	7.82
10	387.09	5.72	319.56	7.85
40	1729.58	5.04	1458.82	6.95
45	1958.55	4.87	1645.42	6.74

3. THE EXPERIMENTAL COMPRESSOR

An open type screw compressor was chosen as an experimental test compressor to simplify the modelling without hermetic motor. This compressor is a screw compressor with only rolling element bearings to manage a wide range of lubrication conditions. It is also equipped with a vapor injection port (economizer port). However, the final solution of compressor for A2L refrigerants would be a hermetic or semi-hermetic compressor. The basic compressor data are shown on Table 3 along with Figure 1.

4. TEST SET UP AND TEST CONDITIONS

The test set up is displayed in Figure 2. The compressor installed is screw type with no internal oil separator. The external oil separator is added. Water cooled sub-cooler is utilized to keep the sub-cooling to be equal or larger than 10 °F. Two sight glasses are also added after a sub-cooler and before the compressor oil return port. The economizer

Table 3: The basic experimental compressor data

Type	Displacement	Suction to Discharge Volume Ratio	Vapor Injection Volume Ratio*	Speed Range	Lubricant	Oil Separator
	cc/rev	1	1	RPM		
Open Screw	384.76	3.5	1.07	1000–4000	POE ISO 120	External

* The suction volume relative to the volume of the flute when the injection port is in the middle of the flute.

Figure 1: The experimental screw compressor showing suction, discharge, oil injection, and vapor injection

heat exchanger and three mass flow meters—auxiliary (economizer) refrigerant flow meter, main refrigerant flow meter, and oil flow meter—are included. For more accurate data acquisition, the pressures and temperatures are measured at each points in Figure 2. Test conditions are chosen based on the speeds (1000, 2000, 3000 and 4000 rpm) without economizer in Figure 3a and with economizer in Figure 3b. The compressor test rig is a full condensing refrigerant loop, including a brazed plate economizer heat exchanger. The size of the economizer heat exchanger influences the vapor injection pressure to some extent.

5. NUMERICAL COMPRESSOR MODEL

Compressor models can take many forms: from basic empirical map-based models to general-purpose high-fidelity 3D models, with various levels of fidelity in between. The choice of modelling approach should normally be driven by what the model is being used for or what questions it is helping to answer. For example, for system simulations with a given compressor and refrigerant, a map based model may be ideal to help predict system power and capacity. Meanwhile, a compressor manufacturer designing the internals of the compressor may need a more fundamental model with 3D elements to help optimize the detailed compressor design.

In this work, it was desirable for the compressor model to have strong physical basis to enable predictability across refrigerants and over a wide operating envelope, while still having the ability to fit the model using a black box data driven approach. Neither an empirical map based approach nor a full 3D model met both of those criteria. Instead, a modeling approach comprised of lumped physical elements assembled to represent key behaviors was used (Stulgies et al., 2009; Cavalcante et al., 2008). A model was assembled to capture the following key physical phenomena for a suction gas cooled hermetic motor or open scroll/screw compressor with an injection port: pressure drop at suction, discharge, and injection ports; leakage from discharge to suction volumes; mechanical friction; suction gas cooling of a motor; and heat loss to the ambient. A schematic detailing the elements describing the hermetic scroll compressor is shown in Figure 4. For an open compressor, the motor is removed along with the motor loss that is heating the suction gas. The model is built in the Modelica language using the TIL-Suite modeling library (TLK-Thermo GmbH, 2020).

The high level mathematical model will now be described element by element, leaving room for flexibility in the

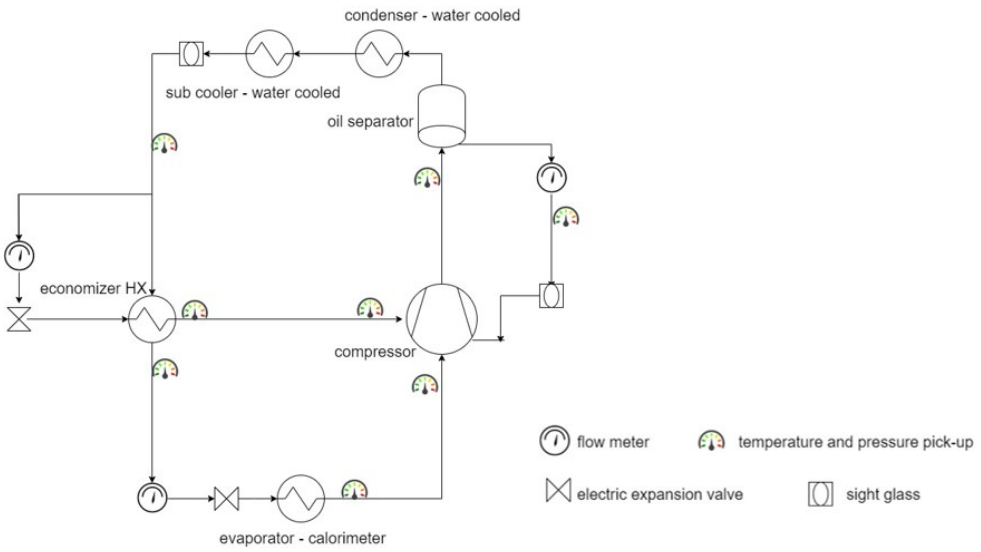

Figure 2: Test Stand Configuration for Economizer Compressor

detailed implementation:

Suction and Discharge Volumes The suction and discharge volume elements are described by constant pressure mixing volumes, for which the 1st law of thermodynamics can be applied:

$$\frac{dU_{\mathrm{CV}}}{dt} = \sum Q_{\mathrm{in}} - \sum Q_{\mathrm{out}} + \sum \dot{m} h_{\mathrm{in}} - \sum \dot{m} h_{\mathrm{out}} \tag{1}$$

Motor The most straightforward approach for modeling the motor is with a constant efficiency. Alternatively, the efficiency could be described as a function of the mechanical torque and speed and other electrical boundary conditions. Given the motor efficiency, the motor can be described by:

$$\eta_{\mathrm{motor}} = \frac{P_{\mathrm{shaft}}}{P_{\mathrm{electric}}} \tag{2}$$

$$Q_{\mathrm{motor,loss}} = (1 - \eta_{\mathrm{motor}})\, P_{\mathrm{electric}} \tag{3}$$

Pressure Drop Elements A semi-empirical orifice model derived from Bernoulli's principle can be used to describe the four pressure drop elements in the compressor model:

$$\dot{m} = A_{\mathrm{eff}} \sqrt{2\rho\Delta p} \tag{4}$$

While the above form is an incompressible formulation, this equation could be further enhanced to consider compressibility effects.

Mechanical Friction In the context of the compressor model, the mechanical friction refers primarily to the fluid viscous dissipation effects internal to the compressor. It is expected to be a strong function of the compressor RPM and should behave within the laminar and turbulent limits. Given these considerations, a reasonable model for the viscous dissipation in terms of the heat generated can be stated as:

$$Q_{\mathrm{friction}} = a \cdot RPM^{n} \tag{5}$$

where a is the friction coefficient and n is expected to be within 1.0 (laminar) and 2.0 (turbulent).

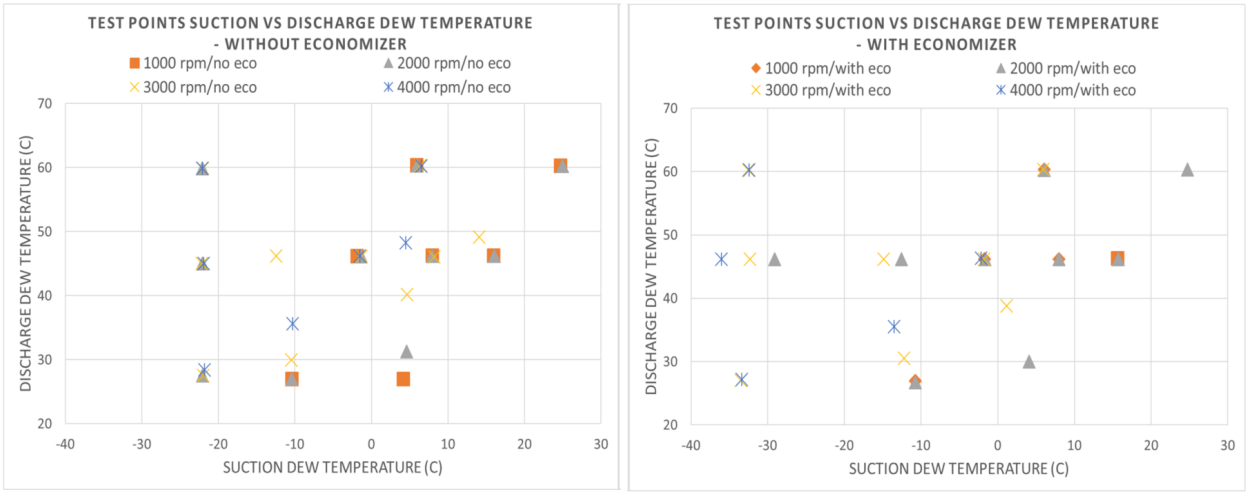

(a) Without Economizer **(b)** With Economizer

Figure 3: Test Points Suction Dew Temperature vs. Discharge Dew Temperature

Shell Heat Transfer For an adiabatic compressor, the discharge temperature will be resolved automatically given the upstream boundary conditions, the mass flow, and the power. However, if more precision is required, then the heat transfer loss through the shell can be considered, which will normally result in a lower discharge temperature. A simple model for the shell heat transfer is to use an overall driving temperature difference with a *UA* conductance coefficient (overall heat transfer coefficient):

$$Q_{\text{shell,loss}} = UA\left(T_{\text{dis}} - T_{\text{amb}}\right) \tag{6}$$

Ideal Compressor The ideal compressor element internal to the complete compressor model can be considered as lossless except for the losses that the compressor has no practical means to avoid, such as losses associated with mixing (due to the mainstream mixing with the injected stream) and the over/under-compression. Depending on the effects considered and where and how the mixing effect is implemented, the specifics can take various forms with up to three parameters: the displacement, the displacement ratio (effective displacement ratio between suction and injection locations), and the built-in volume ratio (or compression ratio, the volume ratio between suction and discharge locations). As an example, if the mixing effect occurs at the injection pressure level in a constant pressure mixing volume with no over/under-compression effects considered, then the following describes the ideal compressor model:

$$\dot{m}_{\text{suc,int}} = \rho_{\text{suc,int}} \frac{RPM \cdot displacement}{60} \tag{7}$$

$$\dot{m}_{\text{dis,int}} = \rho_{\text{mix,int}} \frac{RPM \cdot displacement/displacementRatio}{60} \tag{8}$$

$$\dot{m}_{\text{dis,int}} = \dot{m}_{\text{suc,int}} + \dot{m}_{\text{inj,int}} \tag{9}$$

$$\rho_{\text{mix,int}} = \rho\left(p_{\text{inj,int}}, h_{\text{mix,int}}\right) \tag{10}$$

$$\dot{m}_{\text{dis,int}} h_{\text{mix,int}} = \dot{m}_{\text{suc,int}} h\left(p_{\text{inj,int}}, s_{\text{suc,int}}\right) + \dot{m}_{\text{inj,int}} h\left(p_{\text{inj,int}}, T_{\text{inj,int}}\right) \tag{11}$$

$$P_{\text{shaft,ideal}} = \dot{m}_{\text{suc,int}}\left(h\left(p_{\text{inj,int}}, s_{\text{suc,int}}\right) - h\left(p_{\text{suc,int}}, T_{\text{suc,int}}\right)\right) + \dot{m}_{\text{dis,int}}\left(h\left(p_{\text{dis,int}}, s_{\text{mix,int}}\right) - h\left(p_{\text{inj,int}}, h_{\text{mix,int}}\right)\right) \tag{12}$$

The complete compressor model used in this work used 10 parameters in total that can affect the steady state result (the four A_{eff} values, *UA*, *displacement*, *displacementRatio*, *compressionRatio*, *a*, and *n*). While more details could be added element by element to increase the number of parameters, care must be taken since the model becomes more difficult for an optimizer to fit robustly. By focusing on just the key physical elements with simple physical descriptions, the model has the ability to predict the compressor behavior robustly.

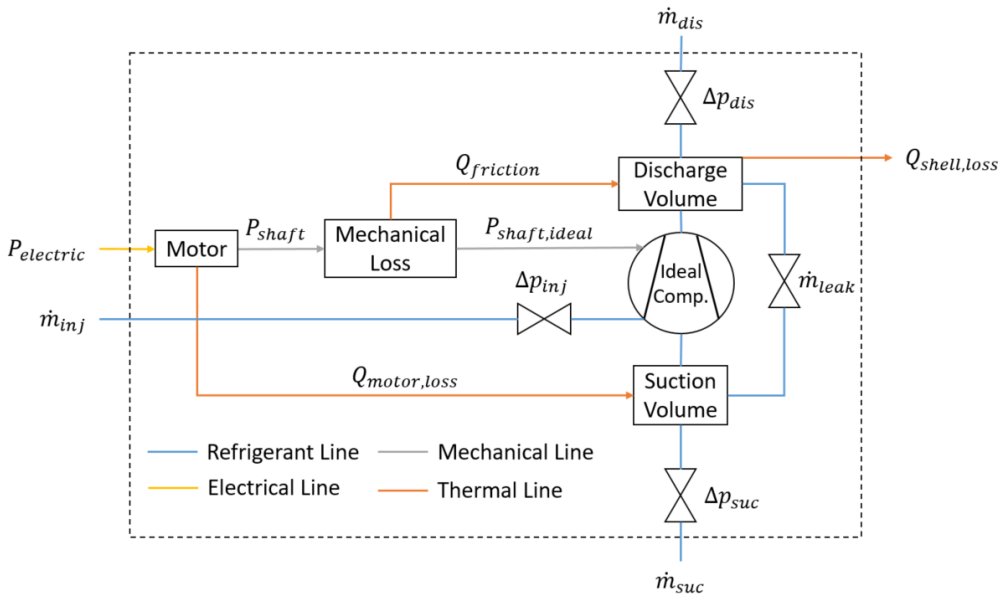

Figure 4: Schematic Model of a Hermetic or Open Scroll/Screw Compressor with Vapor Injection

Given the complete model and test data, a nonlinear optimization tool can be used to fit the parameters. The minimization function must first be defined. For many map based models, there are effectively multiple fits: a fit describing the power and a fit describing the mass flow as an example. In contrast, here there is only one fit, which is conceptually correct since in an actual physical compressor, any elemental physical changes will generally affect mass flows, power, and discharge temperature simultaneously. Therefore the objective function (minimizing the residual sum of squares (RSS) for the test conditions detailed in Figure 3) can be defined as follows:

$$RSS = \sum_{i=1}^{n} \left[\frac{\left(\dot{m}_{\mathrm{suc},i} - \hat{\dot{m}}_{\mathrm{suc},i}\right)^2}{\sigma^2_{\dot{m}_{\mathrm{suc}},i}} + \frac{\left(\dot{m}_{\mathrm{inj},i} - \hat{\dot{m}}_{\mathrm{inj},i}\right)^2}{\sigma^2_{\dot{m}_{\mathrm{inj}},i}} + \frac{\left(P_i - \hat{P}_i\right)^2}{\sigma^2_{P,i}} + \frac{\left(T_{\mathrm{dis},i} - \hat{T}_{\mathrm{dis},i}\right)^2}{\sigma^2_{T_{\mathrm{dis}},i}} \right] \tag{13}$$

Note that the hat symbol (as in $\hat{x}$) denotes the model prediction. It is important for the user to give reasonable estimates for the variance terms, especially since the measurement data have different units and uncertainty levels. Finally, starting guesses are given for each parameter, and the best fit can now be performed. In this work, the Levenberg-Marquardt optimizer was used. After the fit process is completed, various sanity checks are made and the goodness of fit is assessed. The process can be sensitive to the assumed variances and the initial guesses. Often, multi starting guesses are needed to find the minimum. Additionally, it is critical to have a good sized dataset over a large portion of the operating map with many levels in each of the independent variables (typically pressures and speeds on a compressor test stand).

6. NUMERICAL COMPRESSOR MODEL VALIDATION

The compressor test data with R513A refrigerant is used to fit different compressor physical parameters. For the fixed compressor displacement, the independent variables such as compressor suction pressure and temperature, vapor injection port inlet pressure and temperature, and discharge pressure are the required inputs for the fitting process along with the dependents compressor suction mass flow rate, vapor injection mass flow rate, compressor shaft power and discharge temperature. Compressor physical parameters such as areas of the suction valve, the discharge valve, the economizer port, leakages, the displacement ratio and the built-in volume ratio predict the refrigerant mass flow rates through the suction and vapor injection port, combined with additional frictional parameters which predict the compressor shaft power. *UA* captures the heat loss from the compressor shell which directly relates to the compressor discharge temperature prediction.

Table 4 provides the details of the compressor individual fitting targets for the dependents which are based on the compressor test data. The finished compressor fitting process with the individual fitting targets (σ, standard deviation)

has resulted in the following R2 (R, Residual) and RMSD (Root Mean Square Deviation) values, which indicates that there is a very good match with that of the test data. Figure 5a provides the comparison of the simulation vs test data for the compressor suction mass flow rate. Figure 5b provides the comparison of the simulation vs test data for the vapor injection mass flow rate. It can be seen that the injection mass flowrate prediction is not very smooth as compared to the suction mass flow rate, which indicates many factors may have influence on the same. Figure 5c compares the compressor shaft power where the predictions are in very good agreement for the entire operating map. Figure 5d compares the compressor discharge temperature, which is within ±5 K over entire data set excluding a few points.

Table 4: Compressor Fitting Targets and Statistics

Dependent	σ	R^2	RMSD
Suction Mass Flow Rate	0.0009 kg/s	0.9978	5.320×10^{-3} kg/s
Vapor Injection Mass Flow Rate	0.003 kg/s	0.9653	3.843×10^{-3} kg/s
Compressor Shaft Power	99 W	0.9961	2.702×10^{2} W
Discharge Temperature	0.97 K	0.9533	3.476×10^{0} K

Once the compressor physical parameters are finalized based on the fitting process, the parameter based compressor model can now be used to predict the performance when integrated with a refrigeration system with any other refrigerants. In this paper, the original low pressure refrigerant R513A can be replaced with low GWP medium pressure refrigerants R454A or R454C, which are R452A refrigerant alternatives.

7. RESULTS

A system model is set up to run the simulations at AHRI 540-2019 standard rating conditions stated in the Table 5, with R454A and R454C refrigerants. For the medium rating condition where the suction dew temperature is −10 °C and the discharge dew temperature is 45 °C, simulations are performed both with and without economizer (vapor injection). For the low rating condition where the suction dew temperature is −35 °C and the discharge dew temperature is 40 °C, simulations are performed only with the vapor injection because the dew temperature difference between the suction and the discharge is large. The effect of the temperature glide on the thermal performance in the evaporator and the condenser are not considered since there are no physical evaporator and condenser in the simulations.

Table 5: AHRI SI Rating Conditions

Dependent	Low	Medium
Suction Dew Temperature (°C)	−35	−10
Suction Superheat (K)	10	10
Discharge Dew Temperature (°C)	40	45
Condenser Subcooling (K)	0	0
Ambient Temperature Surrounding Compressor (°C)	20	20
Economizer Superheat (K)	10	10
Compressor Speed (rpm)	1000, 2000, 3000, 4000	1000, 2000, 3000, 4000
Refrigerant Name	R454A, R454C	R454A, R454C

Figure 6a shows the capacity ratio between R454C and R454A (i.e. Cooling $\text{Capacity}_{\text{R454C}}$/Cooling $\text{Capacity}_{\text{R454A}}$) at both the rated conditions at different compressor operating speeds. It can be seen that the capacity ratio is typically in the range 0.82–0.86 indicating that the refrigerant R454C requires a larger compressor displacement or a higher compressor speed to match the capacity. It could also be seen that the capacity ratio decreases slightly as the compressor speed is increased. Figure 6b shows the COP ratio of R454C and R454A (i.e. $\text{COP}_{\text{R454C}}/\text{COP}_{\text{R454A}}$) with the increase in the compressor speed. It can be seen that the refrigerant R454C has slight advantage over R454A at lower speeds at low rating condition and it decreases as the speed is increases. At the medium rating condition, the refrigerant R454C has slight advantage over R454A, and the difference is reduced as the compressor speed is increased. Figure 6c shows the difference between the compressor discharge temperatures between R454A and R454C (i.e. $T_{\text{dis,R454C}} - T_{\text{dis,R454A}}$).

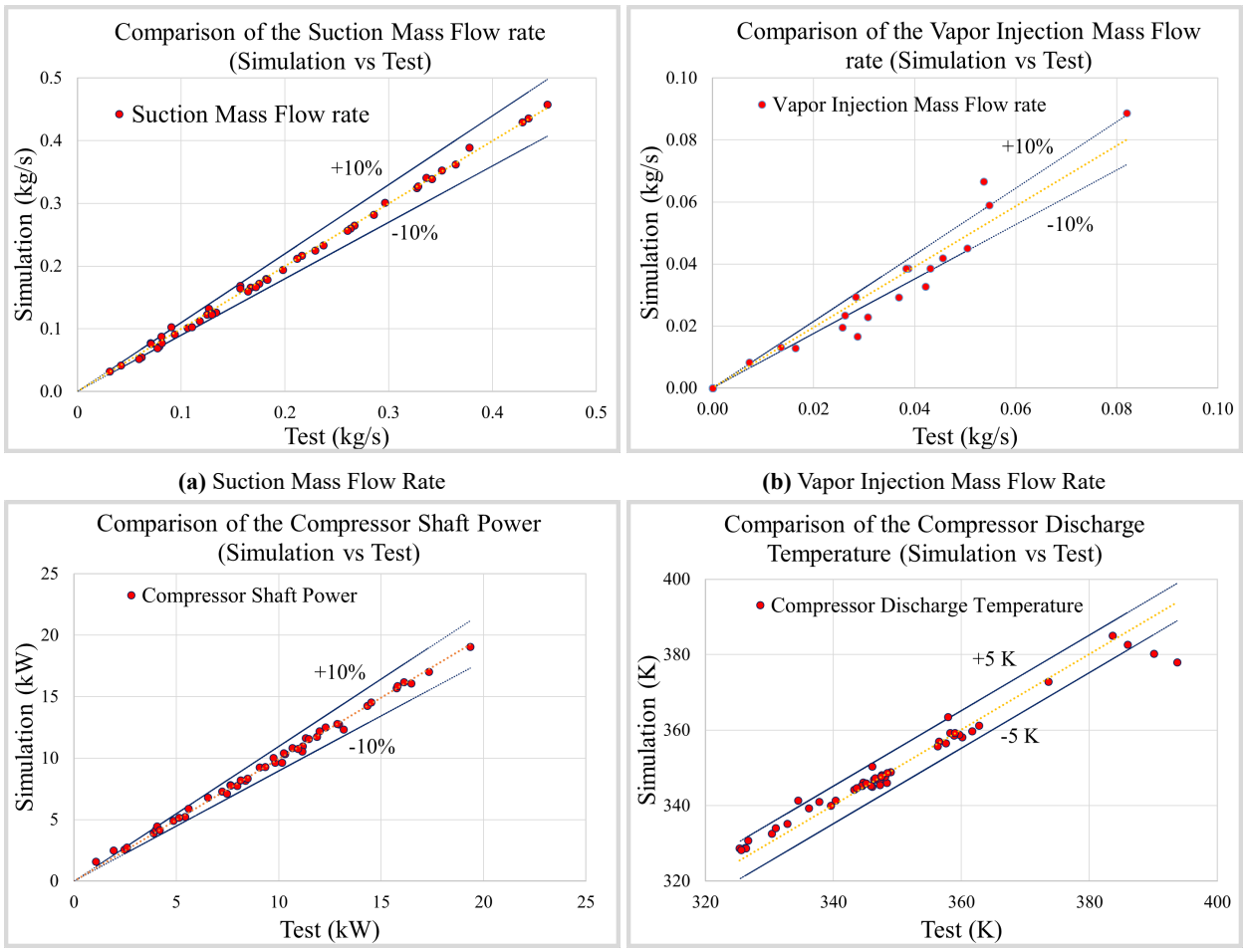

(a) Suction Mass Flow Rate

(b) Vapor Injection Mass Flow Rate

(c) Shaft Power

(d) Discharge Temperature

Figure 5: Simulation vs. Test Comparison

Since the refrigerant R454A has higher mass fraction of R32 in the mixture composition compared to R454C, it always has significantly higher compressor discharge temperature which may require liquid refrigerant injection as a mitigation option. The difference is observed to be larger for −35/40 °C (suction dew temperature/discharge dew temperature) condition compared to −10/45 °C condition. Figure 6d shows the COP ratio with economizer and without economizer (i.e. $COP_{\text{with eco}}/COP_{\text{without eco}}$) for both refrigerants at low and medium temperature conditions. It can be seen that there is an improvement of the COP by about 15 % with an economizer. The COP ratio also decreases as the compressor speed is increased.

8. CONCLUSION

The compressor performance prediction utilizing a numerical physical bulk model with R454A and R454C is conducted using vapor injection with economizer heat exchanger based on compressor test data with R513A. Following findings are observed:

- R454A always gives higher capacity than R454C at the same compressor displacement and speed (Figure 6a).
- R454A gives higher COP than R454C at frozen conditions and higher speeds while R454C gives higher COP at lower speeds for the same frozen conditions (Figure 6b).
- R454C gives always higher COP at fresh conditions independent of speed (Figure 6b).
- R454C gives always lower discharge temperature than R454A (Figure 6c).
- Both refrigerants are expected to need liquid injection to cover the entire application. The proportion of the

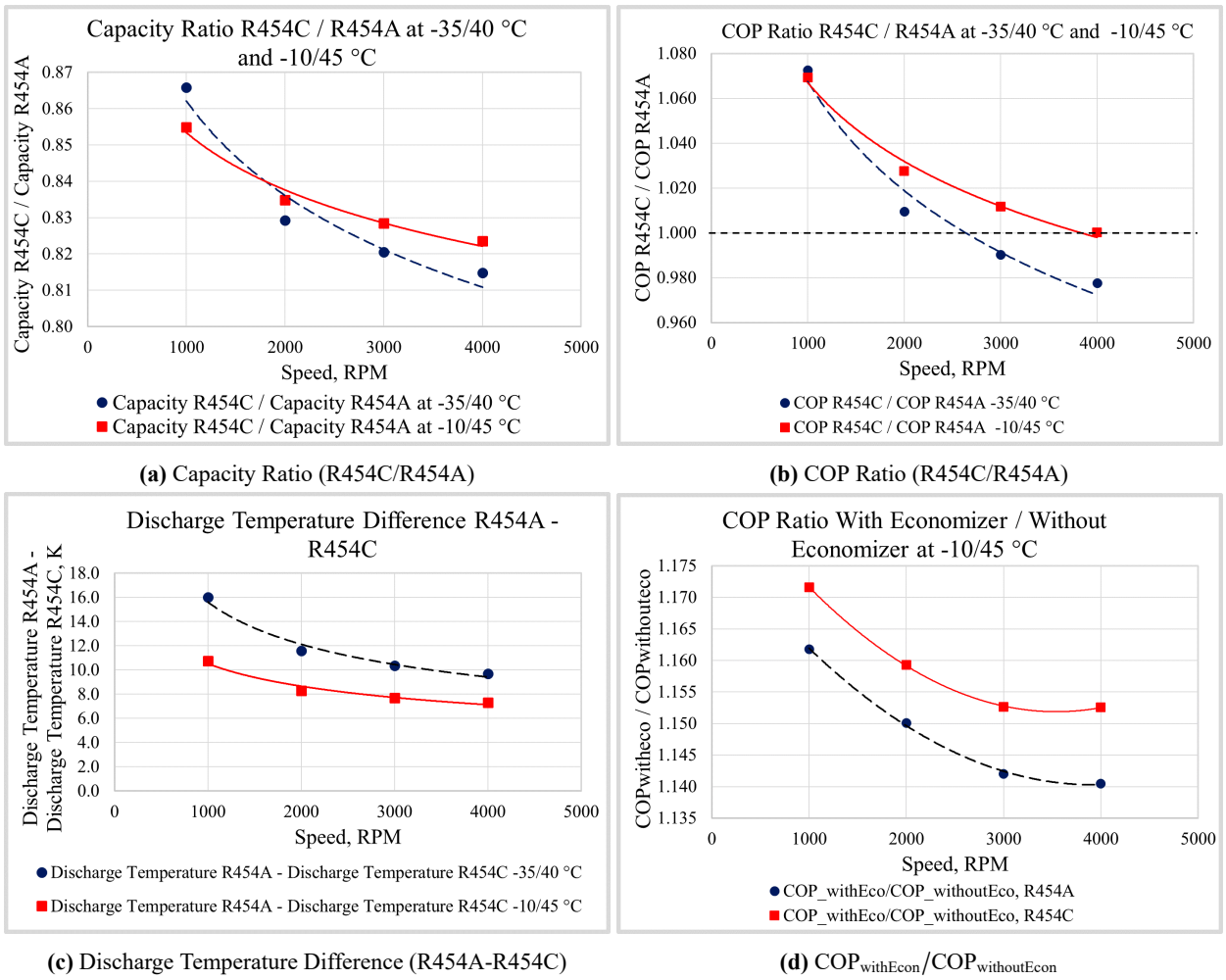

(a) Capacity Ratio (R454C/R454A)

(b) COP Ratio (R454C/R454A)

(c) Discharge Temperature Difference (R454A-R454C)

(d) $COP_{withEcon}/COP_{withoutEcon}$

Figure 6: Comparison Between R454C and R454A

entire application requiring liquid injection will be larger with R454A compared to R454C.

- The benefit of using vapor injection with R454C is greater than R454A (Figure 6d).
- Additional system performance studies will be required for better understanding of R454A vs. R454C applications.

NOMENCLATURE

A_{eff}	effective area	(m^2)	Δp	pressure difference	(Pa)
$\dot{m}$	mass flow rate	(kg/s)	η	efficiency	(1)
h	specific enthalpy	(J/kg)	ρ	density	(kg/m^3)
p	pressure	(Pa)	σ_x^2	variance	($[x^2]$)
P	power	(W)			
Q	heat flow rate	(W)			
s	entropy	(J/(kg K))			
t	time	(s)			
T	temperature	(K)			
U	internal energy	(J)			
UA	overall heat conductance	(W/K)			

Subscript

amb	ambient	int	internal ideal compressor
CV	control volume	leak	leakage
dis	discharge	mix	mixed state
in	inflow	out	outflow
inj	injection	suc	suction

REFERENCES

AHRI. (2020). *Ahri standard 540 for performance rating of positive displacement refrigerant compressors and compressor units* (Standard). Arlington, VA, USA: Air-Conditioning, Heating, and Refrigeration Institute.

Cambio, M. (2016). Representation of a positive displacement compressor map with vapor injection. In *Ashrae annual conference seminar 13: Advances in compressor design, testing, and performance modeling for new efficiency standards and alternate refrigerants.* Orlando, FL, USA.

Cavalcante, P., Farsterling, S., Tegethoff, W., Stulgies, N., & Köhler, J. (2008). Transient modeling and sensitivity analysis of a controlled r744 swash plate compressor. In *International compressor engineering conference.* West Lafayette, IN, USA.

Erickson, L. (1998). Rating equation for positive displacement compressors with auxiliary suction ports. In *International compressor engineering conference.* West Lafayette, IN, USA.

Hundy, G., & Vittal, R. (2000). Compressor performance definitions for refrigerants with glide. In *International compressor engineering conference.* West Lafayette, IN, USA.

Sjoholm, L., & Ma, Y. (2018). A study of low gwp refrigerants for transport refrigeration based on hermetic scroll compressors with an economizer. In *International compressor engineering conference.* West Lafayette, IN, USA.

Stulgies, N., Gräber, M., Tegethoff, W., & Försterling, S. (2009). Evaluation of different compressor control concepts for a swash plate compressor. In *Proceedings of the 7th international modelica conference.* Como, Italy.

TLK-Thermo GmbH. (2020). TIL Suite (Version 3.8.0) [Computer software]. Braunschweig, Germany.

ACKNOWLEDGMENT

The authors wish to thank the management of Trane Technologies and Thermo King for permission to publish this paper. The authors also wish to thank Bruce Wynn, Ken Schultz and Robert Isaacs for supporting this work.